Proceedings of the Nineteenth (2009) International Offshore and Polar Engineering Conference
Osaka, Japan, June 21-26, 2009

ISBN 978-1-880653-53-1 (Set); ISSN 1098-618

Numerical Modelling of 3D Oblique Waves by L-type Multiple Directional Wave Generator

Ruey-syan Shih[1], Chung-ren Chou[2], Wen-kai Weng[2]
1. Tungnan University, Taipei County, TAIWAN, China
2. National Taiwan Ocean University, Keelung, TAIWAN, China

ABSTRACT

The improvements on the oblique planar wave train in a basin generated by multiple irregular wave generators are investigated numerically in this study. Though oblique waves of any desired incident angle can be generated by serpentiform wave generators as they were settled in a single line, the generations of waves are limited in specific areas in the basin, which the effective experiment area with uniform wave field is narrow; therefore, most landforms and/or model are located too close to the wave generators. In this study, numerical simulations of desired oblique waves are generating separately but simultaneously by the two series of serpent type wave generators set in L-shape to enlarge the effective experiment area. Based on the Lagrangian description with time-marching procedure, a three-dimensional multiple directional wave basin was developed to simulate ocean waves by using the BEM with quadrilateral elements. The simulations of perpendicular waves are executed in the first instance to verify the scheme, and proceed with the generations and propagations of oblique waves in larger angle. Accordingly, the comparison of waveforms variation confirms the estimation of oblique waves a feasible scheme.

KEY WORDS: Boundary element method; quadrilateral element; 3D wave basin; serpent-type wave generator; oblique wave.

INTRODUCTION

To evaluate wave impact on coastal structures, the variations of oceanic physical characteristics must be accurately predicted, e.g. the deformation of wave profile, distribution of wave pressure and the velocities of water particles. Studies of wave-wave and/or wave-structure interactions can be carried out either physically in a wave basin or numerically with 3D numerical model field experiments, accordingly, numerous investigations on 2D and 3D numerical models regarding the simulation of nonlinear waves were enthusiastically established in virtue of the considerably high-speed development of science and technology of electronic calculator during the last two decades, the capability of generating multidirectional waves using the snake principle has been investigated for nearly half a century, but only in the past two decades are they widely used to study these problems numerically in three dimensional computer algorithms. Even though there have been a large progress in computer technology, development of 3D numerical wave tank in practical application have still been an arduous task so far due to its considerable quantities of arithmetic units, i.e., computational workload and memory requirement, therefore, simulations of fully nonlinear waves in three dimensional models are still in straitened circumstances, they are generality restricted to two dimensions, consequently, 2D models have been extensively used for the simulations of higher nonlinear water waves at the beginning. Since the propagating directions and the amplitudes as well as the periods of waves in real sea are quite unorganized, model tests in multi-directional three dimensional wave basins are undoubtedly necessary; hence over the last few years, challenging works are ongoing and continuous efforts are made to develop practical three dimensional NWTs. Multidirectional wave can be generated by a serpent type wave generator according to the basic of linear wave maker theory (Dean and Darlymple) of each segment. Practical application of this theory with reality is the generator so-called “snake-type” or “serpent-type” wave generator in a physical laboratory. Unidirectional as well as multidirectional waves can be generated spatially by the sinusoidal motion and by the basic of the “snake principle” of the segments of a serpent-type wave generator, respectively. The incident waves are generated by prescribing motions as a series of piston wave makers.

3D NWTs have been used by Xu and Yue (1992) to simulate multidirectional steep waves and their nonlinear interactions with 3D bodies. A THOBEM 3D-model based on the potential theory and perturbation procedure was developed by Boo et al. (1994) for the simulation of linear and nonlinear Stokes 3rd-order irregular waves, the applications of the 3D-NWT were first verified by the studying of the reciprocal effect between wave and stationed obstacles. Three dimensional fully nonlinear waves and wave-body interactions was also studied in a 3D numerical wave tank (NWT) by Celebi et al. (1998) using desingularized boundary integral equation method (DBIEM) and mixed Eulerian and Lagrangian (MEL) scheme. By using a number of wave-makers as absorption facility, a method for active absorption of multidirectional waves in a 3D numerical wave tank model (NWT) has been present by Skourup and Schäffer (1998) based on a traditional 2D active absorption method, i.e. 2D-AWACS (active wave absorption control system). Furthermore, a finite-difference scheme combined with a modified marker-and-cell (MAC) technique was initially developed for the investigation on the characteristics of non-linear

wave motions and their interactions with a stationary vertical truncated cylinder within a NWT was developed by Park et al. (1999), this scheme was also further extended by Kim et al. (2001) for the study of the characteristic of non-linear multidirectional waves. Analogous scheme with the MEL method was also developed for the investigation of 3D moored floating body motions in fully nonlinear waves using the BEM by Ikeno (2000). Tanizawa and Minami (2001) developed a 3D-NWT model for the simulation of running modified Wigley hull motions in waves by HOBEM.

Though there are numerous developments of various kinds of 3D numerical scheme presented by many researchers, numerical models as well as physical tests encounter a same problem in a multi-directional wave basin using a bank of serpent type wave generators in a single line, the generations of desired waves are limited in specific areas in the basin which the effective experiment area with uniform wave field is narrow, therefore, most landforms and/or model are located too close to the wave generators, as shown in Fig.1, the reflected waves and the re-reflected waves from the obstacles was unable to be absorbed efficiently, which may cause great inaccuracy to the results. Ito et al. (1996) tried to absorb the reflected multidirectional waves by taking into account both the current and past water elevation data measured in front of the wave paddles. Yet, the ineffective dissipation of reflected waves and the limitation of the effective region in a wave basin and/or 3D numerical model seem to contribute seriously to the deviation, and this perplexity had been enthusiastically discussed lately.

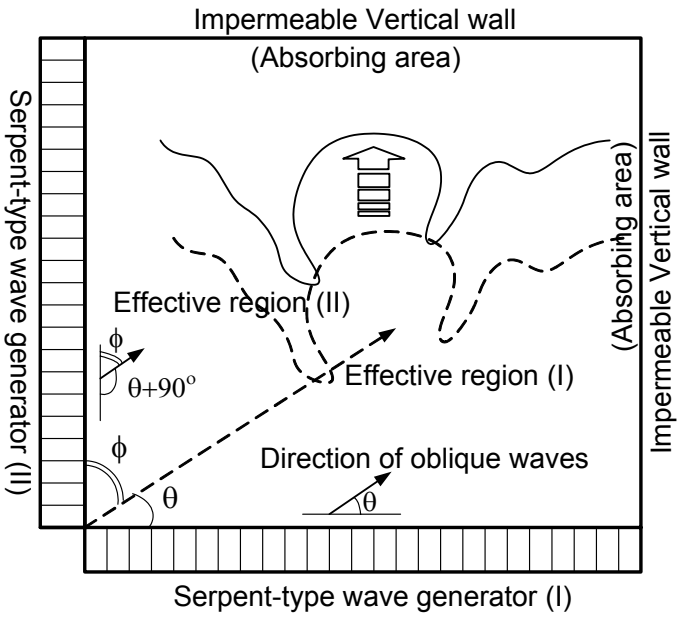

Fig.1 Effective regions in a wave basin

To enlarge the effective experiment area, Funke and Miles (1987) used the partial side walls near the wave generator which as they named it a corner reflector, for the production of oblique waves by the undesirable but intentional reflections, this technique significantly enlarged the effective test area, and move the area beyond the wave board. The directional wave maker theory with side wall reflections developed by Dalrymple was confirmed experimentally by Mansard and Miles (1994), an extensive series of experimental investigations undertaken to further validating the theory of developing a directional wave maker capable of simulating oblique planar wave trains wave was presented. Similar experimental investigations on the applicability and reproducibility of the multi-face generators with small segments have been developed by Hiraishi et al. (1995), the enlargement of the effective test area was investigated experimentally utilizing a multi-face directional random wave maker with generator faces located along the three sides of a basin, this was also known as C-type wave multidirectional wave generator in accordance with its shape (see also Ito et al., 1996). Li and Williams (1998, 2000) provided a complete second-order solution for the three-dimensional wave field, which was produced by the snake-like motion of a wave generators located at one end of a semi-infinite rectangular tank. An optimization method for improving the uniformity of monochromatic oblique waves in a wave basin was adopted by Matsumoto and Hanzawa (1997) using non-linear least square formulation to determine individual paddle motions of a multi-directional wavemaker. A series of multi-segment wave makers are detached and set in L-shape, which was also called as dual-face-snake-type wavemaker (Park et al, 2001). The effects of random wave obliquity and multi-directionality on the wave load are being studied by Yu et al. (2003) performing an extensive 3D model tests in a laboratory. Development of 3D multidirectional wave basin was also studied by Chou et al. (2006) and Shih et al. (2007, 2008) by BEM using a massively parallel computing systems and PC Clusters to solve the unfeasible and complicate computation when using a single PC. In this paper, waves are generated by prescribing adequate snakelike motions at the input boundaries of the segment wave maker, desired oblique waves are generated simultaneously but separately by the two series of serpent type wave generators set in L-shape, which could possibly also be done by generators set in C-shape, prospectively. The algorithm was based on the BEM with linear quadrilateral elements, boundary values are updated at each time step by a forward difference time marching procedure. To overcome the CPU problems, parallel calculation technique on a PC Cluster was adopted for the calculations. However, as mentioned, development of 3D NWT is still a rather tough work, extremely long tremendous computing time and extensive memory capacity is required for a numerical model by means of three dimensional BEM to solve the problems directly in time domain since the influence matrix should be set up and inverted at each time step as the nodes on the free surface moves to new positions. Nevertheless, it is believe that the innovation and great advancement of computer science nowadays would overcome these difficulties before long.

THEORETICAL BACKGROUND AND FORMULATION

2.1 Theoretical Development

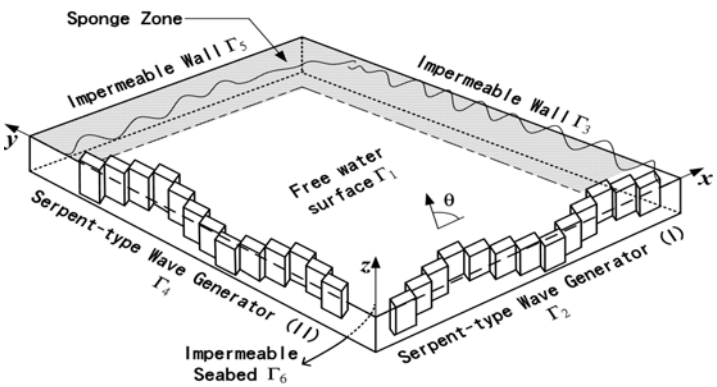

Fig.2 Definition sketch

As shown schematically in Fig.2, the origin is located on the still water surface with the z-axis pointed positively upwards, y-axis positively onward and x-axis positively right. Vertical wall is adopted at the right and opposite bank of the basin so as to bear more resemblance to the physical wave generation. Numerical wave basin is confined in a region

composed of a two serpent type wave generators, Γ_2 , Γ_4 , located individually to the left back corner i.e. the original, at the undisturbed free water surface, Γ_1 , an impermeable vertical wall, Γ_3 , Γ_5 and bottom, Γ_6. Boundaries are bounded and discretized as linear quadrilateral elements. Fluids within the region are conventionally assumed as incompressible, inviscid, and irrotational. The velocity potential $\Phi(x,y,z;t)$ must satisfies the following Laplace equation:

$$\frac{\partial^2\Phi}{\partial x^2}+\frac{\partial^2\Phi}{\partial y^2}+\frac{\partial^2\Phi}{\partial z^2}=0 \tag{1}$$

At the undisturbed free surface, the following nonlinear kinematic and dynamic boundary conditions can be expressed in the Lagrangian form as:

$$u=\frac{Dx}{Dt}=\frac{\partial\Phi}{\partial x} \tag{2}$$

$$v=\frac{Dy}{Dt}=\frac{\partial\Phi}{\partial y} \tag{3}$$

$$w=\frac{Dz}{Dt}=\frac{\partial\Phi}{\partial z} \tag{4}$$

$$\frac{D\Phi}{Dt}+g\eta-\frac{1}{2}\left[\left(\frac{\partial\Phi}{\partial x}\right)^2+\left(\frac{\partial\Phi}{\partial y}\right)^2+\left(\frac{\partial\Phi}{\partial z}\right)^2\right]+\frac{P}{\rho}=0 \tag{5}$$

where $D(.)$ is the total derivative; g, η , and ρ denotes the gravitational acceleration, the surface fluctuation, and the fluid density; u, v, and w are, respectively, the component of the velocity of water particle in x-axis, y-axis and z-axis directions. Notice that P is the gauge pressure on the free water surface and is assumed to be constant (i.e. P=0) on the non-absorbing area.

Since the boundaries of the vertical walls, referred to as Γ_3 and Γ_5, as well as the stationary bottom boundary, Γ_6, are impermeable, the particle velocity on the normal direction is null, therefore:

$$\frac{\partial\Phi}{\partial n}=0 \quad , \quad on \;\; \Gamma_3 \;,\; \Gamma_5 \;\; and \;\; \Gamma_6 \tag{6}$$

where n is the unit outward normal vector. Requirement of continuity between horizontal velocity $U(t)$ of pseudo wave paddle and the fluid particles, the boundary condition on the wave-paddles is obtained through:

$$\frac{\partial\Phi}{\partial n}=-U(j;t) \quad , \quad on \;\; \Gamma_2 \;\; and \;\; \Gamma_4 \tag{7}$$

where j represents the number of wave paddles.

2.2 Algorithm and Differencing Scheme

The boundary value problem for the velocity potential is solved by the boundary integral equation based on the Green's second identity, the velocity potential at any point within the region can be obtained by using the velocity potential $\Phi(\xi_x, \xi_y, \xi_z;t)$ and its normal derivative $\partial\Phi(\xi_x, \xi_y, \xi_z;t)/\partial n$ on the boundaries, the corresponding 3D free space Green's function is defined as:

$$\alpha\cdot\Phi(x,y,z;t)=\int_\Gamma\left\{\frac{\partial\Phi(\xi_x,\xi_y,\xi_z;t)}{\partial n}G(\varsigma,\chi)-\Phi(\xi_x,\xi_y,\xi_z;t)\frac{\partial G(\varsigma,\chi)}{\partial n}\right\}d\Gamma \tag{8}$$

$$\alpha(\chi)=\begin{cases}1 & inside\;\; the\;\; fluid\;\; domain\\ 1/2 & on\;\; the\;\; smooth\;\; boundary\\ 0 & outside\;\; the\;\; fluid\;\; domain\end{cases}$$

$$G(\varsigma,\chi)=\frac{1}{4\pi r} \tag{9}$$

$$\frac{\partial G(\varsigma,\chi)}{\partial n}=\bar{G}(\varsigma,\chi)=\frac{-1}{4\pi r^2}\frac{\partial r}{\partial n} \tag{10}$$

$$\chi=(x,y,z) \tag{11}$$

$$\varsigma=(\xi_x,\xi_y,\xi_z) \tag{12}$$

$$r=|\varsigma-\chi|=\sqrt{(\xi_x-x)^2+(\xi_y-y)^2+(\xi_z-z)^2} \tag{13}$$

The linear quadrilateral element was being adopted in this study, the simplest quadrilateral element is defined by its four corner points, the location of each nodes within the element need to be transform Cartesian (x, y, z) to homogeneous coordinate (ξ_1, ξ_2, η) by conformal mapping process, as shown in Fig.3, where ξ_1, ξ_2, and η are, respectively, the three directions corresponding local coordinate x, y and z.

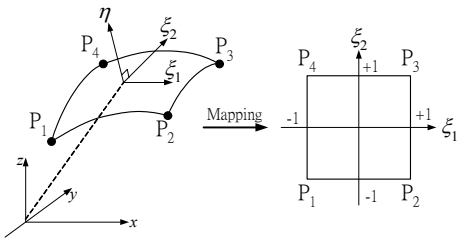

Fig.3 Conformal mapping process of coordinate transformation

$$\Phi(\xi_x,\xi_y,\xi_z;t)=\sum_{k=1}^{4}\Psi_k\Phi_k(\xi_x,\xi_y,\xi_z;t) \tag{14}$$

where
$$\begin{cases}\Psi_1=\frac{1}{4}(1-\xi_1)(1-\xi_2)\\ \Psi_1=\frac{1}{4}(1+\xi_1)(1-\xi_2)\\ \Psi_1=\frac{1}{4}(1+\xi_1)(1+\xi_2)\\ \Psi_1=\frac{1}{4}(1-\xi_1)(1+\xi_2)\end{cases} \tag{15}$$

2.3 Evaluation of Domain Integrals

Consider the development of a 3-D model, the domain was bounded by six boundaries, therefore eq.(8) can thus be rearranged and written as:

$$\alpha\Phi(x,y,z;t)+\sum_{P=1}^{6}\int_{\Gamma_p}\Phi(\xi_x,\xi_y,\xi_z;t)\bar{q}*dA=\sum_{p=1}^{6}\int_{\Gamma_p}\bar{\Phi}(\xi_x,\xi_y,\xi_z;t)q*dA \tag{16}$$

The integral representation of the solution for the Green function may be written for the boundary which has been discretized into N_p (p=1~6) linear quadrilateral element, thus:

$$\alpha\Phi_i(x,y,z;t)+\sum_{P=1}^{6}\sum_{j=1}^{N_p}\sum_{s=1}^{4}h_{ij}^{s}\Phi_j(\xi_x,\xi_y,\xi_z;t)=\sum_{p=1}^{6}\sum_{j=1}^{N_p}\sum_{s=1}^{4}g_{ij}^{s}\overline{\Phi}_j(\xi_x,\xi_y,\xi_z;t) \tag{17}$$

$$h_{ij}^{s}=-\frac{1}{8\pi}\int_{-1}^{1}\int_{-1}^{1}N_s\frac{1}{r^2}\frac{\partial r}{\partial n}\Big|G\Big|_{\Gamma_{ij}}d\xi_1 d\zeta_2 \qquad (s=1\sim4) \tag{18}$$

$$g_{ij}^{s}=\frac{1}{8\pi}\int_{-1}^{1}\int_{-1}^{1}N_s\frac{1}{r}\Big|G\Big|_{\Gamma_{ij}}d\xi_1 d\zeta_2 \qquad (s=1\sim4) \tag{19}$$

r represents distance alone the source, i, and the evaluated point over integrated segment, j.

2.4 Boundary Conditions on wave paddles

The 3-D numerical rectangular wave basin of constant water depth h contains two series of segmented wave generators occupied one wall of 54 segmented wavemakers long and another of 54 segmented wavemakers width as shown schematically in Fig.2, the width of each waveboard is selected as w=0.5h, each segmented generator can be similarly threatened as that in a 2D NWT, i.e., in accordance with the continuity of the horizontal velocities of the wave paddle and that of adherent water particles, the velocities are extrapolated at the interface with approximately without distinction between the wave paddle and fluid. To simulate the oscillating motion of the arrayed wave makers in a physical wave basin (e.g. the serpent type wave generator in NTOU, National Taiwan Ocean University) may be a rather difficult job for numerical model due to the discontinuous phase motion between each wave board, yet this can be solve by considering each node as a hinge that links the detached segments (wave boards), as shown in Fig.4. Waves are generated separately by the two series of serpent type wave generators, though they were set in L-shape, the validation undertaken in this study is to put the theories to the proof, particularly the possibility of the continuity of produced wave crest lines. The elevation of free water surface is related to the velocity potential resembling in a 2D-NWT, i.e. it converts velocity to wave height, the relation between the velocities of wave-generators and the characteristics of the generated waves can be illustrated by the basic of wave maker theory (Dean and Darlymple, 1984). For multidirectional wave generation, it was clarified through the physical experiments that oblique waves can be generated by setting difference phases between adjacent segments, a numerical serpentiform motion is also established likewise by prescribing the velocities based on the fluid particles velocities of water wave theory with a series of piston-type wave generators, and the velocities on the wavemaker boundary for the generation of any desire wave form are therefore described as fellow:

1. For periodical wave generation, the velocities of the first (along x-axis) and second series (along y-axis) generators are given by:

$$U_1(x,t)=\zeta_0\,\alpha(f)\,\sigma\sin(\sigma t-kx\cos\theta) \tag{20}$$

$$U_2(y,t)=\zeta_0\,\alpha(f)\,\sigma\sin(\sigma t-ky\sin\theta) \tag{21}$$

$$\alpha(f)=\frac{\sinh kh\cosh kh+kh}{2\sinh^2 kh} \tag{22}$$

Where angular frequency $\sigma=2\pi f$, f denotes the frequency, ζ_0 is the incident wave height, k is the wave number, h is the water depth, θ is the angle of incident wave and $\alpha(f)$ the transfer function.

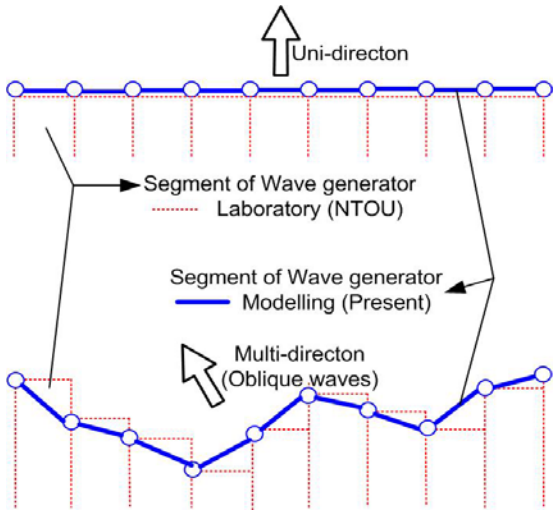

Fig.4 Motion of the arrayed wave makers in a physical wave basin and present numerical model

2. For solitary wave, the velocities can be given as:

$$U_1(x,t)=\zeta_0\sqrt{\frac{g}{h}}\cdot\sec h^2[\sqrt{\frac{3\zeta_0}{4h^3}}C(t-t_c)-x\cos\theta] \tag{23}$$

$$U_2(y,t)=\zeta_0\sqrt{\frac{g}{h}}\cdot\sec h^2[\sqrt{\frac{3\zeta_0}{4h^3}}C(t-t_c)-y\sin\theta] \tag{24}$$

$$C=\sqrt{g(h+\zeta_0)} \tag{25}$$

where g, C, and θ are the gravitational acceleration, wave celerity, and the angle of incident wave, respectively. t_c is a characteristics time scale, which is defined as half the time of the stroke.

3. For unidirectional irregular wave, the velocities can be given as:

$$U_1(x,t)=\sum_{n=1}^{N}\sqrt{2df S_o(f_n)}\cdot\sigma_n\cdot\cos(\sigma_n t-kx\cos\theta-\varepsilon_n) \tag{26}$$

$$U_2(y,t)=\sum_{n=1}^{N}\sqrt{2df S_o(f_n)}\cdot\sigma_n\cdot\cos(\sigma_n t-ky\sin\theta-\varepsilon_n) \tag{27}$$

$$\sigma_n=2\pi f_n \tag{28}$$

$$S_0(f)=0.257H_{1/3}^2T_{1/3}^{-4}f^{-5}\exp[-1.03(T_{1/3}f)^{-4}] \tag{29}$$

$$S(f)=\alpha(f)^2\cdot S_0(f) \tag{30}$$

where $H_{1/3}$, $T_{1/3}$, f , ε_n, and N denotes respectively the significant wave height, associate significant wave period, the frequency, a random variable number between 0~2π and the total number of sampling.

4. For multidirectional irregular wave, the velocities can be written as:

$$U_1(x,t)=\sum_{n=1}^{N}\sqrt{2df S_o(f_n)}\cdot\sigma_n\cdot\cos(\sigma_n t-k_n x\cos\theta_{f_n}-\varepsilon_n) \tag{31}$$

$$U_2(y,t)=\sum_{n=1}^{N}\sqrt{2df S_o(f_n)}\cdot\sigma_n\cdot\cos(\sigma_n t-k_n y\sin\theta_{f_n}-\varepsilon_n) \tag{32}$$

$$\theta_{f_n}=h(\theta,f_n) \tag{33}$$

where θ_{fn} denotes the directional spreading function related with the variable angle of incident wave related to the frequency of each component waves.

2.5 Parallel Computing on a PC Cluster

The quantity of nodes on the free water surface requires 81 multiplied by 41 nodes, and further, plus the other five surface's makes an amount of approximately 5914 nodes, and is an arrangement for the matrix of order 5914×5914 when calculating. Since the computational domain continuously changes, the influence matrix must be set up and solved every time step, consequently, the computation generally requires substantial CPU time and iterative solvers, therefore, the modelling of 3D NWT using single personal computer is unfeasible and is being superseded by massively parallel computing systems and PC Clusters; thus, effective parallel programming has become critical to the progression and development of 3D numerical model. The PC cluster we use comprises eight dual Pentium 4 CPU's workstations putting together and interconnected, each of which consists 4 GB of memory, in order to be able to solve the resulting large matrix, parallel matrix factorization algorithm was developed, in which the original inverse matrix was partitioned into 8×8 submatrixes.

NUMERICAL SIMULATIONS AND DISCUSSIONS

3.1 Generation and wave form deformations

The generation, propagation and deformation of regular and irregular waves in a three dimensional wave basin of constant water depth h are simulated, the wave is generated by an array of piston type wave makers oscillating at the constant water depth of h=0.5m, the basin is 20m wide and 40m in length, ζ=0.05m and $\Delta t=T/200$, T denotes the wave period. As mentioned previously, the boundaries, Γ_1~Γ_6, are divided into N_1~N_6 discrete elements, where N_1=4800 (4961 nodes), N_2=120 (183 nodes), N_3=120 (183 nodes), N_4=120 (183 nodes), N_5=80 (123 nodes) and N_6=300 (341 nodes) was selected presently. Although the wave field is produced based on the snake principle, namely that serpent-type wave maker will produce any desired type of waves propagating obliquely to the plane. However, the finite width of the basin with fully reflecting sidewalls results in the wave generations being influenced by sidewall reflections, therefore in this article, the simulations of perpendicular waves are executed in the first instance to verify the scheme, the unidirectional periodical wave propagation was first carried out for simplicity. In order to verified the consecutive wave profiles of desired oblique waves which are generated simultaneously by two separate series of serpent type wave generators set in L-shape, the distribution of the velocities on the x-y planar can thus be obtained as fellow:

1. The variation of the velocity for oblique periodical wave generation:

The simulation of the generations of oblique regular periodical wave utilizing different incident waves angles, 90° and 45°, are shown respectively in Fig.5 and Fig.6 (see Shih, 2007), in which x and y axis denote respectively the tangential direction of the serpent-type wave generator in series 1 and series 2, the distribution of the velocities can be obtained by an equation combining eqs.(20) ~(22) as:

$$U(x,y,t)=\zeta_0\,\alpha(f)\,\sigma\sin(\sigma t-kx\cos\theta-ky\sin\theta) \tag{34}$$

Furthermore, the preliminary modeling result of the generation of periodical wave in a basin using the BEM model is represents in Fig.7, from which we observed that some waves around the x-axis may be rather sharp-pointed, because even though there are 4961 nodes

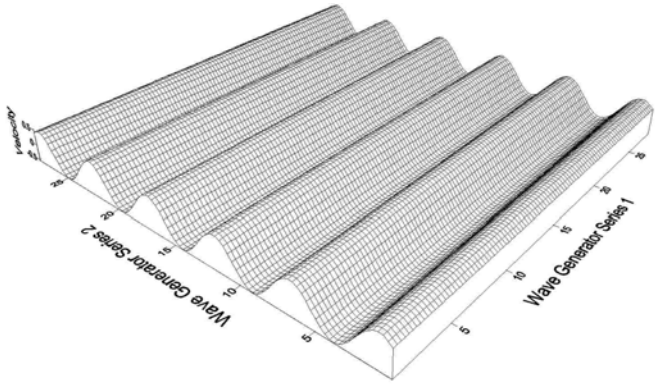

Fig.5 Spatial distributions of velocity in x-y planar for periodical regular waves when θ=90°(Numerical solution).

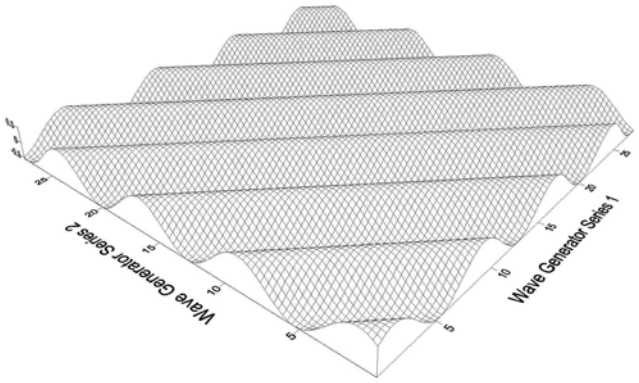

Fig.6 Spatial distributions of velocity in x-y planar for periodical regular waves when θ=45° (Numerical solution).

distributed over the water surface, i.e. 81 multiplied by 41 nodes (40m × 20m in actual size), yet, in terms of the present case h=0.5m, each wave length only comprises not more than 8 nodes in the direction of y-axis, especially near the generator, this number is inadequate for a smooth wave form. Nevertheless, the increasing of nodes also represents the increasing of calculating time and requirements of computer hardware capacity. Hence, development of 3D NWT is still a rather tough work as mentioned, an extremely long tremendous computing time and extensive memory capacity is required for a fully nonlinear time-dependence numerical model.

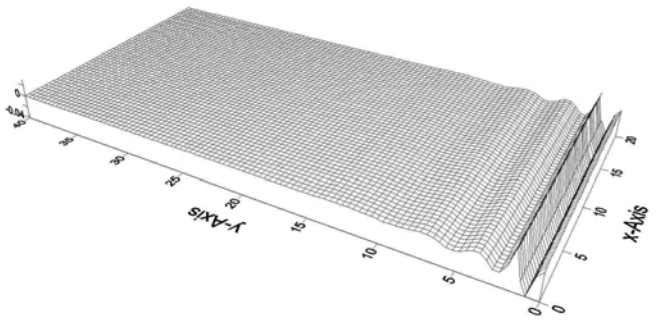

Fig.7 Spatial distributions of wave height in x-y planar for periodical regular waves in a wave basin when θ=90° (Modelling)

2. Distribution of wave height for unidirectional irregular waves:

Random waves are usually a combination of numerous, theoretically unlimited, components of sinusoidal waves. The generation, obliquely propagated of irregular wave in a three dimensional wave basin can be simulated by adopting eqs. (26)~(30) as the governed condition on the wave generator based on the snake principle, spatially sinusoidal motion of a serpent-type wave maker will produce any desired type of waves propagating obliquely to the plane, however, unidirectional random waves comprised various of component waves merely in one single direction, thus, the spatial distribution of wave height in x-y planar to the generations of unidirectional irregular wave perpendicularly is shown in Fig.8.

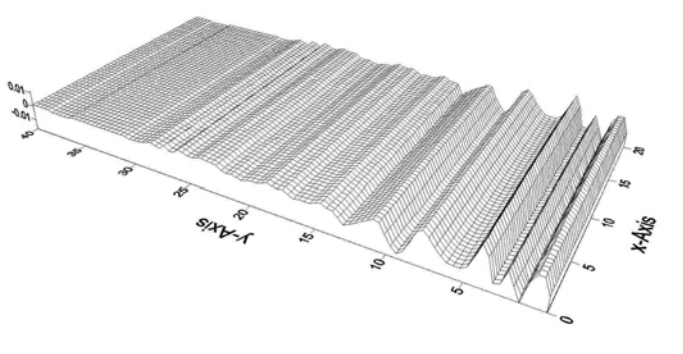

Fig.8 Spatial distribution of wave height in x-y planar for uni-directional irregular waves in a wave basin when θ=90° (Modelling)

3. Distributions of the wave height for multidirectional irregular waves:

As interpreted previously, random waves are commonly an accumulation of numerous components of sinusoidal waves with random phase, this was known as RPHM (Random Phase Spectrum Method), yet, multidirectional random waves are more complicated but realistic about comprising of various monochromatic component waves not only with random phase, different amplitude and frequency, but also in various directions, nevertheless, the spatial distribution of multidirectional wave groups trains exists a target directionality known as the " main wave direction", θ, the measurement of directional spectra can be accomplished by several techniques such as the maximum entropy method (MEM), the Fourier Expansion Method using a cos2 type function (FEMcos) and by using a sech type function (FEMsech) usually apply to wind waves…etc., the spatial distributions of wave height in x-y planar of multidirectional random wave when θ=90° is shown in Fig.9.

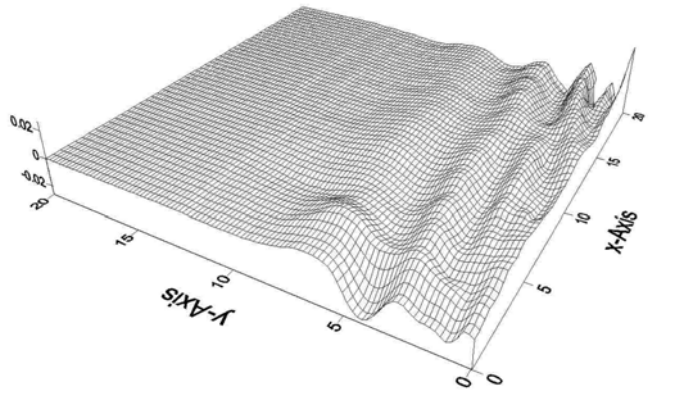

Fig.9 Spatial distribution of wave height in x-y planar for multi-directional irregular waves in a wave basin when θ=90°.

4. Distribution of surface elevation for the generation of solitary wave:

The spatial distributions of velocity in x-y planar to the generations of solitary wave with variable propagation incident directions are shown in Fig.10. Solitary waves are generated by a long stroke motion of piston wave generator in a 2DNWT as well as 3D unidirectional NWT, similarly in a multidirectional 3D wave basin, oblique solitary wave can be generated by a series of stroke motion with a slightly difference in time of each segmented piston, and the motion of each piston is governed by a control signal which is calculate directly by Eqs.(23)~(25).

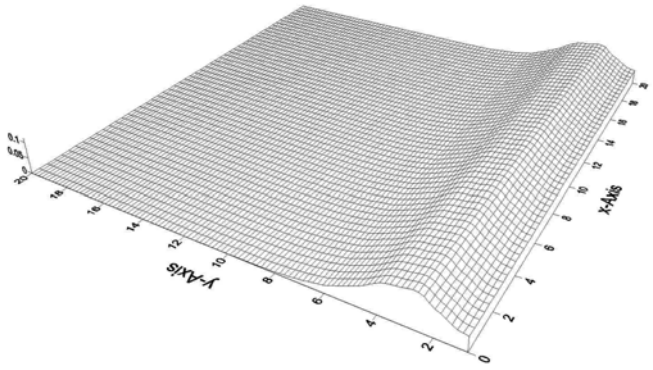

Fig.10 Spatial distribution of wave height in x-y planar for solitary wave in a wave basin when θ=90°.

5. Variations of the wave height for oblique periodical regular waves:

The spatial distributions of velocity in x-y planar to the generations of oblique regular wave in different time steps are shown in Fig.11. In a multidirectional 3D wave basin composed of multi-face serpent type wave generators with individual controlled paddles, the motion of each piston is governed by a control signal calculate directly by Eqs.(20)~(22). Fig.12 shows the action of each segmented generator in series 2 from t=1T~8T(T remains wave period) and the contour map of wave height distributions is also shown in Fig.13, while a conspicuous slight angle can be found in the left back corner near the origin. However, some accurately investigations on the spatial distribution of wave direction and angular spreading of uni- as well as multi-directional wave would be prospectively studied.

3.2 Conservation of mass and energy

The present numerical model was validated through convergence test according to the conservation of energy and mass determined by Eqs.(35)~(38) as respectively shown in Fig.14 and Fig.15, in a oblique periodical wave case, the mass above the still water level is equal to that of the area the paddles have swept (back and forth), mass of a surface can be evaluate by surface integral where η is orientable and n is a unit normal to the surface, else, the total energy is equal to the energy transmitted by the paddles, which slightly increase along with the kinetic energy received from the paddles, however, the total mass on the surface seems to descend progressively as the generation proceeded, the cause of this phenomenon is not yet clear, hence, investigations to this appearance would be carry out anew, prospectively.

$$V(t)=\int_{\Gamma_1}\eta(e_z\cdot n)d\Gamma \qquad \text{(Mass of surface)} \qquad (35)$$

$$E_k=\frac{1}{2}\rho\int_{\Gamma_{1\sim6}}\Phi\frac{\partial\Phi}{\partial n}d\Gamma \qquad \text{(Kinetic energy)} \qquad (36)$$

$$E_p = \frac{1}{2}\rho g \int_{\Gamma_1} \eta^2 (e_z \cdot n) d\Gamma \qquad \text{(Potential energy)} \qquad (37)$$

$$E = E_k + E_p \qquad \text{(Total energy)} \qquad (38)$$

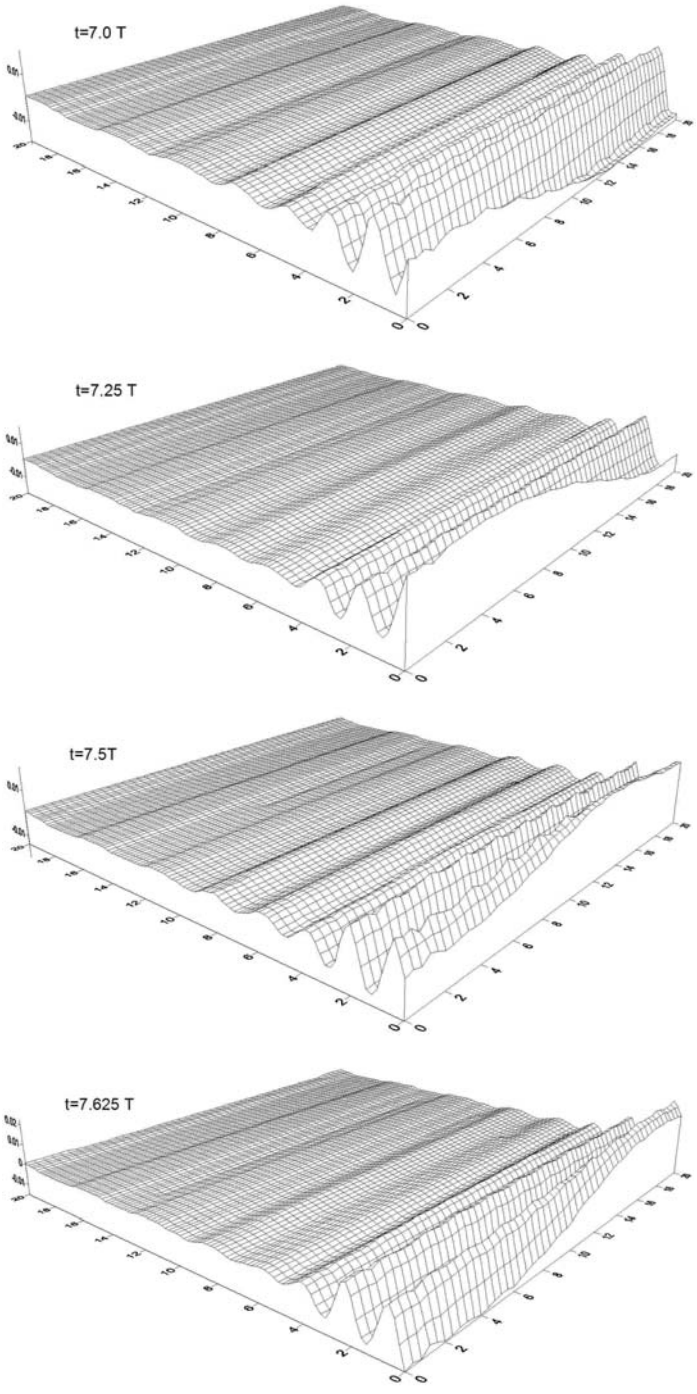

Fig.11 Spatial distributions of wave height for oblique periodical regular waves in a wave basin when θ=80° (T remains wave period).

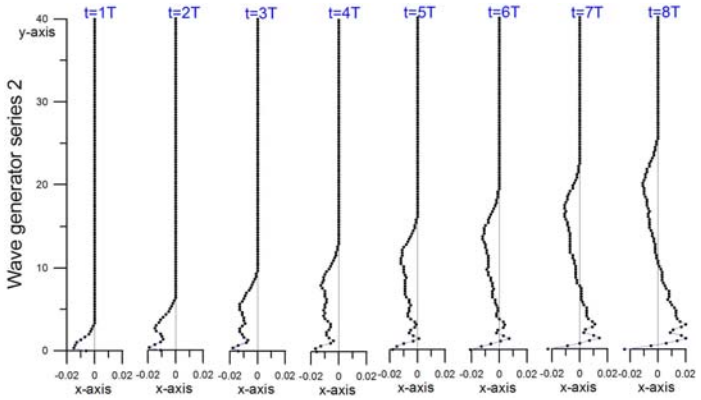

Fig.12 Action of each segmented generator in series 2 when θ=80°.

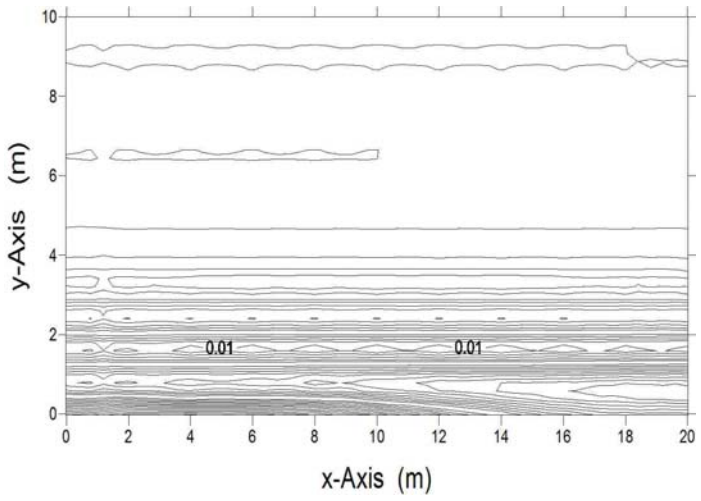

Fig.13 Contour map of wave height distributions for oblique periodical regular waves in a wave basin when θ=80°.

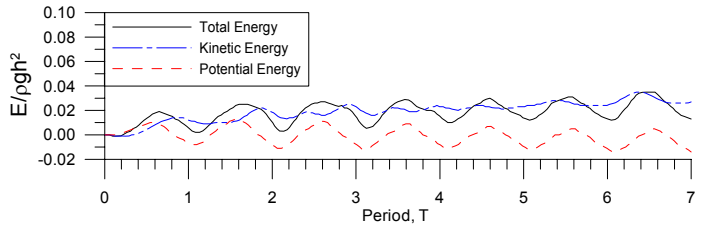

Fig.14 Variation of Energy in the Basin

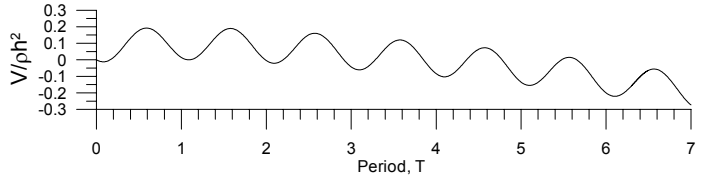

Fig.15 Variation of Total Mass on the surface

CONCLUSIONS

A three-dimensional multidirectional wave basin has been developed to simulate ocean waves using the BEM with quadrilateral elements. Based on the Lagrangian description with time-marching procedure, any desired oblique waves can be generation by two series of serpent type wave generators set in L-shape, the simulations of perpendicular regular, irregular and solitary waves as well as multidirectional random waves are executed, also proceed with the generations and propagations of oblique periodical waves in a small angle, some conclusions are summarized:

1. In this article, the numerical model was developed using the 3DBEM with Lagrangian time marching procedure, and the boundaries was discretized into 5914 linear quadrilateral elements, since the matrix should be set up and inverted at each timp step, a tremendous computing time and extensive memory capacity is required for a fully nonlinear numerical model, it takes almost 2 hours of time interval between each time step, nevertheless, it is believed that the innovation and great advancement of computer science nowadays would overcome these difficulties before long, however, since desired oblique waves are generated simultaneously but separately by the two series of serpent type wave generators set in L-shape, the rudimentary results of the simulations indicate that the present model a feasible scheme.

2. The model was put to the proof by the cases of sinusoidal regular wave, solitary wave, unidirectional as well as multidirectional irregular waves, however, in the oblique periodical regular wave case, the total mass on the surface descend progressively as the generation proceeded, investigations to this appearance should be carry out prospectively, besides, some accurately investigations on the spatial distribution of wave direction and angular spreading of multidirectional wave case would be studied.

3. Impending simulations of the generations and propagations of oblique waves will proceed with larger angles. It can be anticipated that the influence of reflected waves cause by the impermeable vertical wall may cause great errors to the estimations, especially on two extremities sides and edges of the wave generator. Therefore, development of the present conditions on Γ_3 and Γ_5 into a so-called "snake absorber" is imperative and to be consider prospectively.

ACKNOWLEDGEMENTS

The authors wish to express their gratitude for the financial aids of the National Science Council, Republic of China, Project No. NSC-95-2221-E-019-075-MY3(CRC) and NSC-97-2221-E-236-011-(RSS).

REFERENCES

Boo, S. Y., Kim, C. H., and Kim, M. H., 1994, "A Numerical Wave Tank for Nonlinear Irregular Waves by 3D Higher Order BEM," Int. J. Offshore Polar Eng. 4, pp. 17-24.

Celebi, M. S., Kim, M. H. and Beck, R. F., 1998, " Fully Nonlinear 3-D Numerical Wave Tank Simulation", Journal of Ship Research, Vol.42, No.1, pp.33~45.

Chou, C.R., Shih, R.S. and Weng, W.K., 2006, "Development of 3-D Wave Basin by BEM (III) ", Proceedings of the 28th Ocean Engineering Conference in Taiwan, National Sun Yat-Sen University, pp.456~463, Kaohsiung, Taiwan.

Dean, R.G. and Dalrymple, R.A., 1984, "Water Wave Mechanics for Scientists and Engineers", Prentice-Hall, Englewood Cliffs, New Jersey.

Funke, E. R. and Miles, M.D., 1987, " Multi-Directional Wave Generation with Corner Reflectors ", *Technical Report*, National Research Council Canada, Division of Mechanical Engineering, Hydraulics Laboratory.

Hiraishi, T., Kanazawa, T. and Fujisaku, H., 1995, " Development of Multi-Face Directional Random Wave Maker", The 5th International Offshore and Polar Engineering Conference, Vol.3, pp.26~33, Hague, Netherlands.

Ikeno, M., 2000, " A Numerical Model for 3-D Floating Body Motion in Nonlinear Waves Using the BEM", The 10th International Offshore and Polar Engineering Conference, Vol.3, pp.201~208, Seattle, USA.

Ito, K., Katsui, H., Mochizuki, M. and Isobe, M., 1996, "Non-reflected multi directional wave maker theory and experiments of verification", Proc. of the 25th International Conference of Coastal Engineering, pp.443~456.

Kim, M. H., Niedzwecki, J. M., Roesset, J. M., Park, J. C., Houng, S. Y., and Tavassoli, A., 2001, "Fully Nonlinear Multidirectional Wave by 3-D Viscous Numerical Wave Tank", Journal of Offshore Mechanics and Arctic Engineering, Vol. 123, pp.124-133.

Li, W., and Williams, A. N., 1998, "Second-Order 3-D Wavemaker Theory with Side Wall Reflection," Proc. ISOPE'98 Conf., Montreal, Canada, 3, pp.235-241.

Li, W., and Williams, A. N., 2000, "Second-Order Waves In A Three-Dimensional Wave Basin With Perfectly Reflecting Sidewalls", Journal of Fluids and Structures, Vol.14, pp.575-592.

Mansard, E.P.D. and Miles, M.D., 1994, " Experimental Validation of Directional Wave Maker Theory with Side Wall Reflections ", International Journal of Offshore and Polar Engineering, Vol.4, No.4, pp.273~277.

Matsumoto, A. and Hanzawa, M., 1996, " New Optimization Method for Paddle Motion of Multi-Directional Wavemaker ", Proc. 25th Conf. on Coastal Eng., Orlando, FL. USA, Vol.1, pp.479~492.

Park, J.G., Kim, M.H. and Miyata, H., 1999, " Fully Non-linear Free-surface Simulations By A 3D Viscous Numerical Wave Tank ", International Journal for Numerical Methods in Fluid, Vol.29, pp.685~703.

Park, J.G., Uno, Y., Matsuo, T., Sato, T. and Miyata, H., 2001, "Reproduction of Fully-Nonlinear Multi-Directional Waves By a 3D Viscous Numerical Wave Tank ", The 11th International Offshore and Polar Engineering Conference, Vol.3, pp.17~22, Stavanger, Norway.

Shih, R.S., Chou, C.R. and Tsao Y.L., 2007, " Development of Numerical 3D L-type Multiple Directional Irregular Wave Generator (I) ", Proceedings of the 29th Ocean Engineering Conference in Taiwan, National Cheng Kung University, pp.65~70, Tainan, Taiwan.

Shih, R.S. and Chou, C.R., 2008, " Development of Numerical 3D L-type Multiple Directional Irregular Wave Generator (II) ", Proceedings of the 30th Ocean Engineering Conference in Taiwan, National Chiao Tung University, pp.175~180, Hsinchu, Taiwan.

Skourup, J. and Schäffer, H. A., 1998, " Simulations with a 3D Active Absorption Method in a Numerical Wave Tank", The 8th International Offshore and Polar Engineering Conference, Vol.3, pp.107~115, Montréal, Canada.

Xu, H. and Yue, D.K.P., 1992, " Computations of fully-nonlinear 3D water wave ", Proc. 19th Symposium of Naval Hydrodynamics, Seoul, Korea.

Yu, Y.X., Li, B.X. and Zhang, N.C., 2003, " Oblique and Multi-Directional Random Wave Loads on Vertical Breakwaters". China Ocean Engineering, Vol.17, No.2, pp.189~201.